Integrated Petrophysical Evaluation Applied to the Characterization of Shaly-Sand Reservoirs in the Santonian Gas Field, Santos Basin, Brasil*

Thamy da Silva[1] and Marcio Coutinho[1]

Search and Discovery Article #50503 (2011)
Posted October 24, 2011

*Adapted from extended abstract presented as oral presentation at AAPG International Convention and Exhibition, Milan, Italy, October 23-26, 2011.

[1]Petrobras, Rio de Janeiro, Brazil. (thamyd@gmail.com)

Abstract

The integration between new technologies (Natural Gamma-ray Spectrometry log tool, magnetic resonance, etc.), characterization methodologies (probabilistic evaluation, crossplots analysis) and core data (petrophysical and petrological data and sedimentologic description) is very important to identify diagenetic constraints for reservoir quality in shaly-sand reservoirs in order to build a more robust petrophysical model. This work presents a formation evaluation for two main Santonian sequences of an important gas field composed of siliciclastic reservoirs in Santos Basin, eastern Brazilian margin.

In these reservoirs the dispersed clay (mainly chlorite) and the sand composition (rich in feldspar) may complicate the petrophysical analyses when using conventional tools to identify the different reservoir zones, to evaluate the permeability and the saturation model. The basic analyses are not enough for the full comprehension of the constraints on these shaly-sand reservoirs. This work proposes an integrated workflow using the core-log approach to improve the characterization of rocks and fluids. This method will allow the understanding of the factors which affect petrophysical properties, as well as identify using log curves the main petrofacies described, applying all available information, the core data and spectral gamma ray tools in order to build a multi-mineral model.

The NGS logs and crossplots element ratios have been highly important to the identification and evaluation of these reservoirs. The probabilistic approach has shown significant results for the mineralogical model which was supported by core and plug data. The saturation model has been fitted to the resonance saturation curve calibrated in laboratory (T2 cutoff) and the porosity and permeability models were adjusted with plug data. Finally, the crossplot NGS ratio has proved to be a useful tool assisting in the identification of petrofacies through clusters analysis. The adopted approach has indicates that chlorite was one of the factors that affected the quality of the reservoir (mainly permeability), but did not affect resistivity curves. Moreover, this approach has also proved that those dispersed clays can be identified using the NGS logs and that their volume can be safely calculated with the probabilistic (multi-mineral) model. All these analyses have provided a more predictive model to be applied in a field in the early developmental stage.

Introduction

The presence of chlorite, clay mineral formed through diagenetic processes, is recognized in the Santonian reservoirs of the Santos Basin. The occurrence of this clay mineral in sandstones intervals in the well studied affects the characteristics of petrophysical properties (permeability and porosity) of the reservoirs and suggests the necessity for a detailed petrophysical evaluation. Integrating rock and log curves as well as the use of special log curves (NGS, NMR) can provide a better characterization of complex reservoirs, as well as providing a more robust petrophysical model.

In these reservoirs the presence of chlorite, as dispersed clay, may compromise the petrophysical evaluation, when conventional methods are used for calculating water saturation. In addition, the very low permeability make difficult determine the irreducible water saturation using the conventional methods. This work presents a formation evaluation that applied all available petrophysical and petrological data in order improve the petrophysical model in terms of fluid and rock.

The analysis of the well presented in this paper covers two main areas of a Santonian age siliciclastic reservoir in a field located in the central region of the Santos Basin.

Location

The Santos Basin is located entirely offshore in the southeastern, part of the Brazilian Continental Margin, along the coast of the states of São Paulo, Rio de Janeiro, Paraná and Santa Catarina. It covers 352,260 km^2 and is one of the largest Brazilian sedimentary basins. The basin is limited to the south by the Florianópolis High which separates it from the Pelotas Basin, and to the north by the Cabo Frio High, which separates it from the Campos Basin. (Freitas et.al. 2006). The area target of this work is located in the central portion of the Santos Basin (Figure 1).

Geological Context and Petroleum System

The Santos Basin has its origins with the opening of the Atlantic Ocean during the Cretaceous. The Rift Sequence of the Santos Basin occurred between 130 and 114 Ma and was a result of extensional process, forming half-grabens filled by continental lacustrine sediments. The sedimentary filling of this basin is characterized, in general, for three main phases of deposition: Rift Sequence (continental and lacustrine sedimentation plus volcanic), Transitional Sequence (lagoon-lake sedimentation) and Drift Sequence (marine neritic sediments, bathyal and abysmal).

The deposition in the Santos Basin had begun in the Neocomian within a paleoclimate context with highly dry and anoxic events in subaqueous environments.

The onset of continental drift and the consequent removal of the center oceanic spreading changed the profile of the basin that evolved from an evaporitic context, which dominated during the Aptian, to a marine environment. The geological record of this phase was divided into two units that represent the different sequences within the Drift Sequence (Mohriak and Cainelli, 1999). At the base a Sea Restricted Supersequence (essentially carbonate) and above it an Open Sea Supersequences (mainly siliciclastic).

The Open Sea Supersequence is characterized for a stratigraphy strongly influenced by tectonic movements on the continent and numerous rearrangements of the drainage patterns, which influence directly the supply and distribution of terrigenous facies along the basin. The reservoirs rocks presented in this paper are siliciclastic reservoirs, within the context of the Santonian Open Sea Supersequences (Ilha Bela Member, Itajaí-Açú Formation) (Figure 2).

The Rift Sequence of the Santos Basin contains the main hydrocarbon source rocks, source to the rift and drift sequences reservoirs. The Lower Cretaceous lacustrine shales, called Guaratiba Formation are located at great depths and are in the gas generation window. The hydrocarbons from the Guaratiba Formation lacustrine shales (source rock) were accumulated preferentially in marine sandstones of the Itajaí-Açú Formation. Marine shales deposited in deep water seal these hydrocarbons. (Chang et.al. 2004) The traps can be stratigraphic, structural and mixed. The migration of hydrocarbons occurs through faults (listric faults associated with tectonic salt; discordance surfaces and salt windows) and carrier-beds. (Freitas et. al., 2006)

Classification and Zonation of the Reservoir

The sandstones of the Ilhabela Member (Itajaí-Açú Formation) were deposited within an elongated channel, generated by halocinesis during the deposition of Albian carbonates (Freitas et. al., 2006). These sandstones are classified as Arcosian (Folk, 1968), with essentially volcanic lithic fragments (Sombra et al., 1990, in Anjos et.al., 2003). The area subject of this study is interpreted as resulting of deposition processes from high-density hyperpycnals flows associated with a river system under catastrophic floods (Davila et. al., 2005, Souza and Dias Filho, 2007). Probably, these processes are not efficient to separate the different fractions of sediments and consequently there is a mixture of sand and clay fractions.

Internally these reservoirs are divided into two stratigraphically well correlated zones. (Coutinho et al., 2007) These zones are treated here as Upper and Lower Zones. They are separated by a continuous layer of shale of about seven meters. (Figure 3) The Lower Zone is divided into four sub-zones whose boundaries were established through changes in density log curve, while the Upper Zone is divided into three sub-zones, bounded by thin layers of shale (Coutinho et. al., 2007). These zones are easily identified and separated using magnetic resonance curves and the curves of density and neutron porosity.

According to the petrographic reports in the Upper Zone of this well the reservoirs are characterized by presenting his clay matrix composed entirely by chlorite, while in the base, called here as Lower Zone, the reservoirs are characterized by presenting chlorite, illite, illite/smectite and other diagenetic constituents, especially where the intergranular clay is absent (i.e., calcite, quartz, K-feldspar, dolomite, albite, pyrite, and titanium oxide). Quartz and feldspar occur forming cement, while the other constituents may occur by replacing the framework grains.

The Lower Zone base (the sub-zones called R7 and R6) presents, in addition to clay, a higher concentration of quartz-feldspathic cement, which reduces their porosity and permeability. The increase in cement is reflected in the density curve, which shows higher values in these sub-zones (Figure 3). This reservoirs in general presents intermediate to low values of porosity and low a very low permeabilities and the permeabilities values rarely exceed 10mD.

Petrophysics Analysis of Clay Reservoir

The method of determining water saturation (Sw) was designed by Archie (1942) for reservoirs composed by clean sandstone with high resistivity.

$$Sw = \sqrt[n]{\frac{Rw \cdot a}{Rt \cdot \phi^{m}}} \quad (1)$$

Where:

Sw= Water saturation;
Rw = Resistivity of formation water;
m= Cementation coefficient or porosity exponent;
n= Saturation exponent;
a= Constant derived empirically;
Rt =Formation resistivity;
f =Porosity

This limitation had as result some variations of this equation in order to determine water saturation in reservoirs with more complex characteristics, such as shaly-sand reservoirs. Some of the most popular models to determine water saturation were Waxman-Smits Model (Waxman and Smits, 1968) and Dual Water Model (Clavier, 1977). These models consider the electrical properties of clays in the formation (Asquith and Krygowski, 2004). Dual Water Model predicts the presence of two electrically different waters in the clay structure, one irreducible water closer the clay grain surface (dispersed clay), called bound water (Sw_b) and a mobile water that can be displaced by hydrocarbons (free water).

$$\frac{1}{Rt} = \frac{\phi_T^{\,m} \times Sw_T^{\,n}}{a} \times \left[\frac{1}{Rw} + \frac{Sw_b}{Sw_T} \left(\frac{1}{Rw_b} - \frac{1}{Rw} \right) \right] \quad (2)$$

Sw_t = Total water saturation;
Sw_b = Bound water saturation;

m = Cementation coefficient or porosity exponent;
n =Saturation exponent;
a = Constant derived empirically;
Rt = Formation resistivity;
Rw_b = Bound water resistivity

Hilchie (1978 in Asquith and Krygowski, 2004) noted that the greatest impact of clay is decrease the resistivity contrast between oil, gas and water zones making very difficult to determine the production zone. However, this author suggests that this effect is only significant when the clay volumes are higher than 15%. To apply the saturation model that includes clay is more important to determine the values of clay resistivity than their volume. The clay resistivity is directly affected by the cation exchange capacity (CEC). The clay minerals differ in their values of CEC. The kaolinite and chlorite have extremely low values of CEC, while illite and montmorillonite have high CEC values. (Table 1) Therefore, the montmorillonite and illite impact the values of resistivity much more than chlorite and kaolinite (Asquith and Krygowski, 2004).

In the case of chlorites, particularly, they have bound another type of water in their structure, called capillary water, which is retained in the micropores of the crystalline structure of clay. Only the magnetic resonance tools can detect this type of water. The use of a Dual Water Model would not be ideal for this particular case, and may overestimate the values of water saturation. Many of the problems of interpretation occur in formations where the water is not too salty (< 20,000 ppm NaCl). In high salinity formation waters which water has high salinity, clays have less influence in formation resistivity. Therefore, in reservoirs with very salty formation water, to calculate saturation without correction for clay (Archie equation) would be closer to the real water saturation (Asquith and Krygowski, 2004).

Consequently, the water saturation calculation used Archie's equation, because it is a shaly-sand reservoir whose water salinity is much higher than 20,000 ppm NaCl, the resistivity curves show very high values, chlorite is the main clay mineral and NMR data is available to adjust de saturation model.

Log Analysis

In order to build a petrophysical model a probabilistic approach was applied for obtaining the volumes of rock and fluid. The final product of this process was the generation of a volumetric mineralogical model and finally, the porosity and fluid saturation. The input data were obtained from log curves (complete suite of conventional log curves plus NMR and NGS), laboratory reports and other internal reports. These documents provide data of formation water salinity, electrical parameters, irreducible saturation, data from drilling fluid, temperature, pressure data, T2 cutoff from lab (NMR), core and plug analysis (matrix density, porosity and permeability) and petrographic analysis.

The zones were identified using NMR log curves and were separated into three different colors: Upper Zone (orange), Lower Zone (yellow) and Non-reservoir Zone (green) (Figure 3 track 2 and Figure 5, track 1). After analysis of quality control and determination of reservoir zones, were made several crossplots and histograms in order to identify the lithology of the formation, type of matrix, and density.

The clay volume calculation in probabilistic model had as input log curves: density, neutrons, U matrix (from photoelectric factor curve) and spectral gamma ray. The total gamma ray was not considered due the presence of k-feldspar in sandstones that affect the log response.

The diagram RhoMatApp x UmatApp presents a concentration of points that can be interpreted as an effect of arcosian sand. In addition, the diagram Nphi x RhoB indicates the presence of dispersed clay in the matrix (Figure 4 A and B). The NMR curves indicated the presence of free fluid. In order to identify the presence of different fluids in the reservoir, it was made use of a technique called Mvar. The values of *m*, obtained from the equation, when the reservoir is in water zone, can help to identify the different types of porosity present in the intervals.

$$m\text{var} = \frac{-\log\left(\frac{Rt}{rw}\right)}{\log(Phi)} \quad (3)$$

Where:
m_{var} = Cementation Factor,
Rt= Resistivity;
Phi = Porosity;
Rw = Water resistivity

m_{var} = 1,3135 + 25,7256x*Phi* (4)

In addition, the diagram Mvar x Phi can be used to estimate the type of fluid present in the reservoirs through the analysis of the slope (Figure 4 C). The high slope (value greater than 20 in the second term of equation) is indicative of gas zone. Slopes greater than 6 and below than 20 are indicative of oil zones and slopes below 6 are indicative of water zones.

The pressure data confirm the presence of a hydrocarbon zone with gas gradient (Figure 4 D) and no evidence of water contact. The structural position of the well, relative to other wells in the field, over a contact gas / oil or gas / water enhances this evidence. Is important highlight that in reservoirs with low permeability even with capillary pressure data is difficult to establish the irreducible water saturation value, because most of the pore throat have small sizes and even applying high capillary pressure the irreducible water could not be reach. The boundary between irreducible and free water is not so obvious in this kind of reservoirs. In this case is important take into account all the production information and the NMR saturation curve (with T2 cutoff known) can provide valuable information.

The probabilistic model adopted was composed by a simple mineralogical model that considered the most representative minerals described on petrographic reports, that includes a matrix composed by quartz, feldspar, chlorite, calcite and fluid (water and gas). For non-reservoir intervals the model was composed by clay, calcite and water. The model had shown excellent fit with core data. The porosity obtained using this model presented a good fit with the data plug and NMR log curve (Figure 3, track 7).

The saturation model had a better fit with the saturation curve obtained from the magnetic resonance (Figure 5, track 4), that was calibrated with the T2 cutoff obtained in the laboratory (Figure 3, track 13). For the T2 cut off lab determination are taken into account the clay present in the rock samples. (Nascimento, 2006) In order to define the T2 cut off values per zones, were used the most representative values reported by Azevedo et. al. (2007) It was noted that the T2 cut off changes were related with the facies changes (Figure 3, track 10, 11 and 13).

Spectral Log Analysis

One of the applications of natural gamma-ray spectrometry tool (NGS) is determining the type of clay from the analysis of the ratios between the elements Thorium, Uranium and Potassium. The Thorium / Potassium crossplot, the most applied to determine the types of clay, showed that there is a clear separation between upper reservoirs (orange) and the lower reservoirs (yellow) (Figure 6).Considering the petrographic analysis, the reservoirs from the Upper Zones have chlorite as single clay mineral while the Lower Zones also have cement and illite in their composition. The Thorium / Potassium crossplot confirmed it and could be responding to these clays and reservoir quality. In the Upper Zones predominate facies with higher clay content while in the Lower Zones predominate cleaner or cemented petrofacies (Figure 3, track 10 and 11, Figure 7A and B).

This preliminary analysis is important to identify the potential of these curves to identify variations along the well that could be associated with textural changes in the reservoirs, the volume and type of clay and in consequence changes of facies and reservoir quality. Considering the previous petrographic description, an electrofacies model was build. Those previous petrographic descriptions were used to train a neural network that, where the main input is the NGS data curves, with good results (Figure 3 track 10 and 11).

The construction of a neural network for these reservoirs is a challenge due to the subtle changes on these facies related to textural features, selection, type and volume of clay.

Souza and Dias Filho (2007) characterized these reservoirs in terms of petrofacies in order to individualize textural characteristics, diagenetic and petrophysical properties. They defined five petrofacies: A, B, C, D and E. The Petrofacies C and D were divided into C + and C -, D + and D - considering aspects of quality of reservoir.

The Petrofacies A is characterized by the high content of total clay (15 to 20%) mainly chlorite matrix, and localized carbonate cementation, porosity around 15% and permeability lower than 2 mD. The Petrofacies B is an intermediate between the A (high levels of matrix) and C (high levels of fringe). This facies is characterized by massive sandstone, moderate levels of matrix chlorite and an average porosity around 16% and permeability lower than 2 mD (Figure 7A). The Petrofacies C is characterized by fine to medium sandstone with high content of chlorite, low levels of matrix and cement of quartz and feldspar. The Petrofacies C + has better selection and thicker texture and better reservoir quality. The porosity average is 17% and permeability eventually can overcome 10mD. The Petrofacies C - is characterized by well-selected fine sandstones and high levels of chlorite. The porosity average is 15% and permeability is lower than 1 mD. The Petrofacies D is characterized by fine and coarse sandstones, poorly selected. This petrofacies presents cementation by quartz, feldspar and calcite, low

values of chlorite and the presence of discontinuous matrix. The Petrofacies D + shows high content of cement quartz and feldspar. The porosity average is 13% but has a diverse range of permeabilities and can reach high values, together with the Petrofacies C + represent the best reservoir facies. The Petrofacies D - is heavily cemented by quartz, feldspar, and calcite, with higher proportions of calcite cementation. The average porosity is 9% and the permeability is lower than 2mD. The Petrofacies E is represented by fine grained sandstones, rich in illite, and strong cementation of quartz, feldspar, carbonate and chlorite. The average porosity is 10% and the permeability is lower than 0.1 mD (Figure 7B). The control of the permo-porous characteristics of these reservoirs is reflected on petrofacies that had taken into account the stratigraphic, depositional and diagenetic controls on reservoir.

The seven petrofacies (petrofacies and sub-divisions) were used in order to create an electrofacies model.

The crossplots (Th x K) and neural networks shows that spectral curves are relevant as input variable. When just the conventional curves were used to train the neural network the results were not so good (Figure 8). The neural network model was run in different programs in order to compare and get the better results. The better results were reached using a probabilistic neural network model (PNN). The networks were trained with 43% of data, verified with 10% and tested with just 4% of the data. Those networks reproduced quite well the total interval, mainly considering that was used just one well. It is important to note that the facies poor represented (facies A, C - and D +) show the higher error results. They should be trained with more information. Further training applying more core data information from other wells can provide a better adjust, even using other neural network model or better network configurations.

Conclusion

The reservoirs of the field are composed by feldspathic sandstones (arcosian) showed in RhomatApp x UmatApp crossplot. Nphi x RhoB crossplot classified the clay as dispersed in agreement with the core analysis reported.

The Mvar technique used to identify fluid types, showed gas in all reservoir intervals, according with the pressure and production data and structural position relative with other wells. This could be a good technique to apply in wells that does not count with pressure data.

The saturation model applied was the Archie model that does not consider the clay presence and showed very good adjust with saturation by NMR. Probably this is due to the salinity of water formation, which inhibits the clay influence on resistivity response.

The results showed that is possible to reproduce the petrofacies by network techniques when using the correct set of curves. The petrophysical model using probabilistic model presented very good results and reproduced very well the mineralogical and fluid characteristics of the well, that were confirmed though core data, NMR porosity and saturation log curves. The results allow defining the correct input information in the log program and core analysis program, in order to provide the geological model with a facies model and rebuild the petrophysical model per facies with more detail, which will allow to develop the field correctly.

Acknowledgments

The idea of an integrated work does not just come from the integration of data and information; it depends on the integration of ideas and especially the integration of people. I would like to thank PETROBRAS management for allowing the publication of data and colleagues who helped providing data, information and time for discussion. In particular the geologists: Henrique Penteado (E&P-EXP/GEO/GEAT), Paulo Denicol, Carlos Francisco Beneduzi and Antonio Nascimento (E&P-EXP/AFOE/AFP), Rogerio Schiffer de Souza and Dorval Carvalho Dias (CENPES / PEDEXP /GSEP), Sandra Carneiro (UN-BS/ENGP/RES), Guillermo Gonzálvez (Petrobras Argentina), Holden Amorim (INTERTEC) and Adriana Godoi (UNRIO/EXP/AAG).

References

Anjos, S.M.C.; L.F. De Ros, C.M.A. Silva, 2003, Chlorite authigenesis and porosity preservation in the Upper Cretaceous marine sandstones of the Santos Basin, offshore eastern Brazil In: Clay Cements in Sandstones ed. Oxford: IAS Special Publication, Blackwell Scientific Publications 34, p. 291-316.

Archie, G.E., 1942, The electrical resistivity log as an aid in determining some reservoir characteristics: Journal of Petroleum Technology, v. 5, p. 54-62.

Asquith, G., and D. Krygowski, 2004, Log Interpretation, *in* Basic Well Log Analysis: AAPG Methods in Exploration 16, p. 115-135.

Azeredo, R.B. deV., 2007. Determinação de T2 e T1 de corte e análise de RMN do filtrado de fluido de perfuração: Rio de Janeiro PETROBRAS. CENPES.PDP. CT TRA 016/07, 52 p.

Chang, H.K., M.L. Assine, J. Castro, J.S. Tijen, F.L. Fernandes, A.C. Vidal, S.P. Rostirolla, L. Koike, C. Clavier, G. Coates, and J. Dumanoir, 1977, Theoretical and experimental bases for the dual water model for interpretation of shaly sands: Society of Petroleum Engineers, Annual Meeting, paper SPE-6859.

Coutinho, M.R., M.T. Ribeiro, and A. da S. Barroso, 2007, Geodirecionamento e avaliação de poços horizontais utilizando o perfil de ressonância magnética: 7º. Simpósio Técnico de Operações Geológicas, 8 p.

Dávila, R.S., C.V. Madeira, J.L.P. Moreira, S.F. Santos, and D.C. Dias Filho, 2005, Sedimentologic characterization of Santos Basin gas reservoirs: shallow and deep marine siliciclastic depositional systems related to hyperpycnal flows (Brazil deep seds – deep-water sedimentation on the Southeast Brazilian Margin Project):AAPG Bulletin, v. 89 (digital), Program Abstracts.

Freitas, A.F.D., D.B.R. Moreira, E. Perez, F.R.B. de Dios, and T.C.S.D. da Silva, 2006, Bacia de Santos: Estado da Arte. Série Geologia do Petróleo: Bacias Sedimentares Brasileiras: v. i.-PETROBRAS; UERJ. Rio de Janeiro, 73 p.

Folk, R.L., 1968, Petrology of Sedimentary Rocks: Hemphill´s, Austin, TX, 107 p.

Pereira, M.J., and F.J. Feijó, 1994, Bacia de Santos: Boletim de Geociências da Petrobrás, v. 8/1, p. 219 – 234.

Nascimento, J.D.S., R. Beer, R.B. de V. Azeredo, and A.P.M. de Sousa, 2006, Determinação laboratorial do tempo de relaxação transversal de corte para a calibração de perfis de ressonância magnética nuclear: PETROBRAS. CONTEC N-2847, Relatório Interno, PETROBRAS, online at http://www.petrobras.com.br

Souza, R.S., and D.C. Dias Filho, 2007, Petrologia e qualidade de reservatórios dos arenitos santonianos, Bacia de Santos: PETROBRAS. GESEP, RT 013/07. Relatório Interno (internal communication).

Waxman, M.H., and L.J.M. Smits, 1968, Electrical conductivities in oil-bearing shaly sands: Society of Petroleum Engineers Journal, v. 245, p. 107-122.

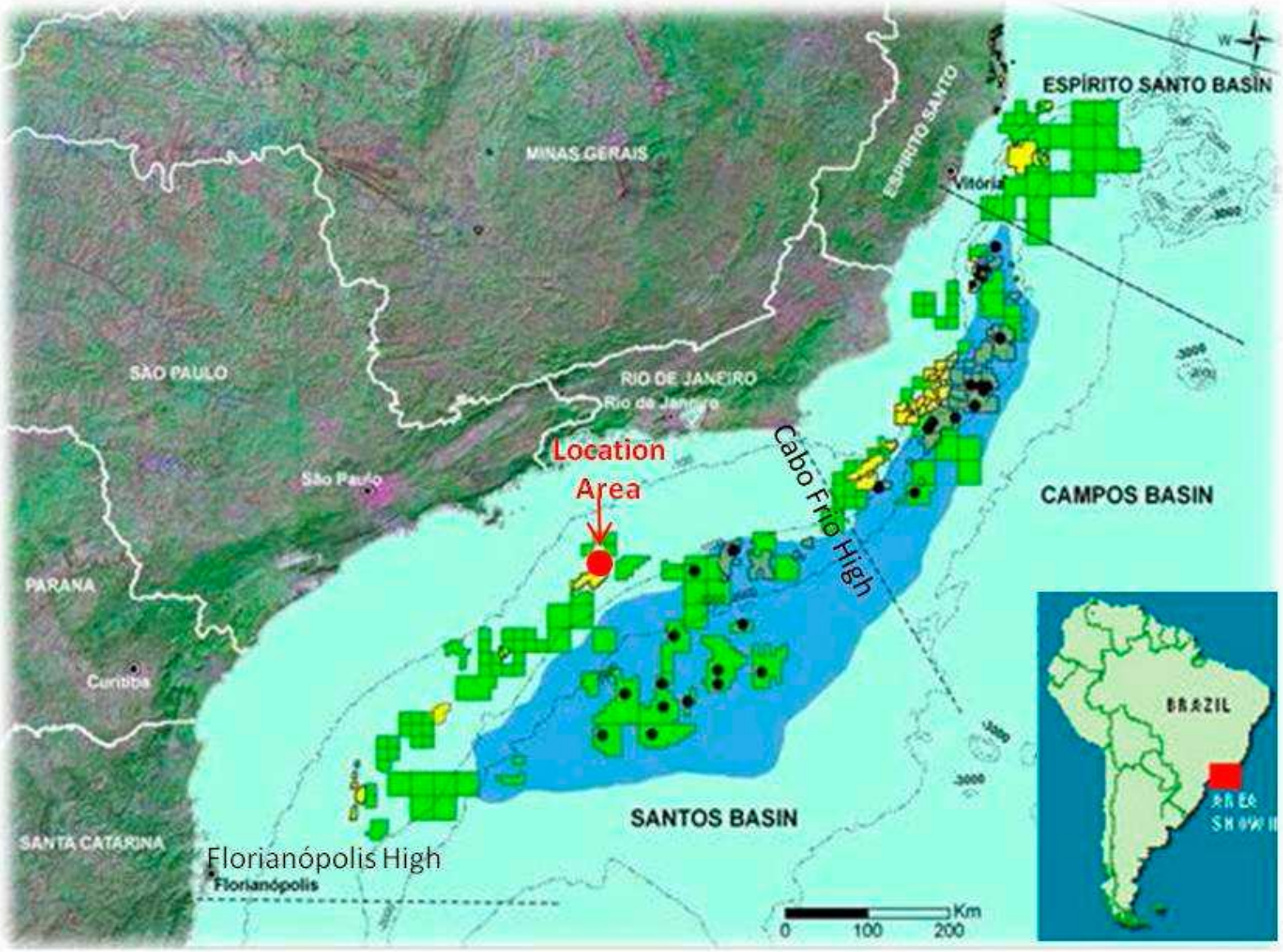

Figure 1. Map of the Santos Basin and location area (source: PETROBRAS webpage).

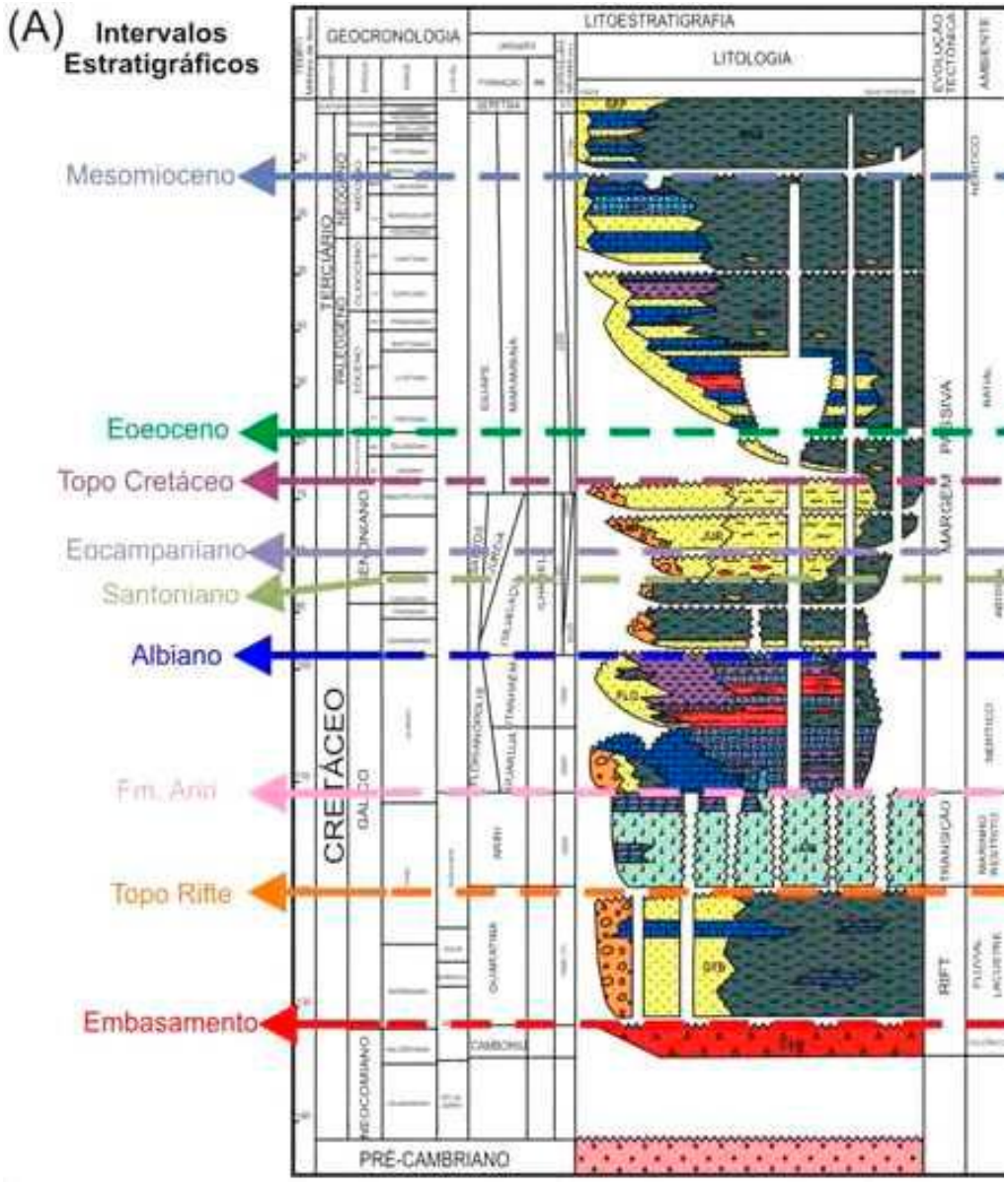

Figure 2. Santos Basin Stratigraphic Chart with Reservoirs study location (Modified of Pereira and Feijó, 1994).

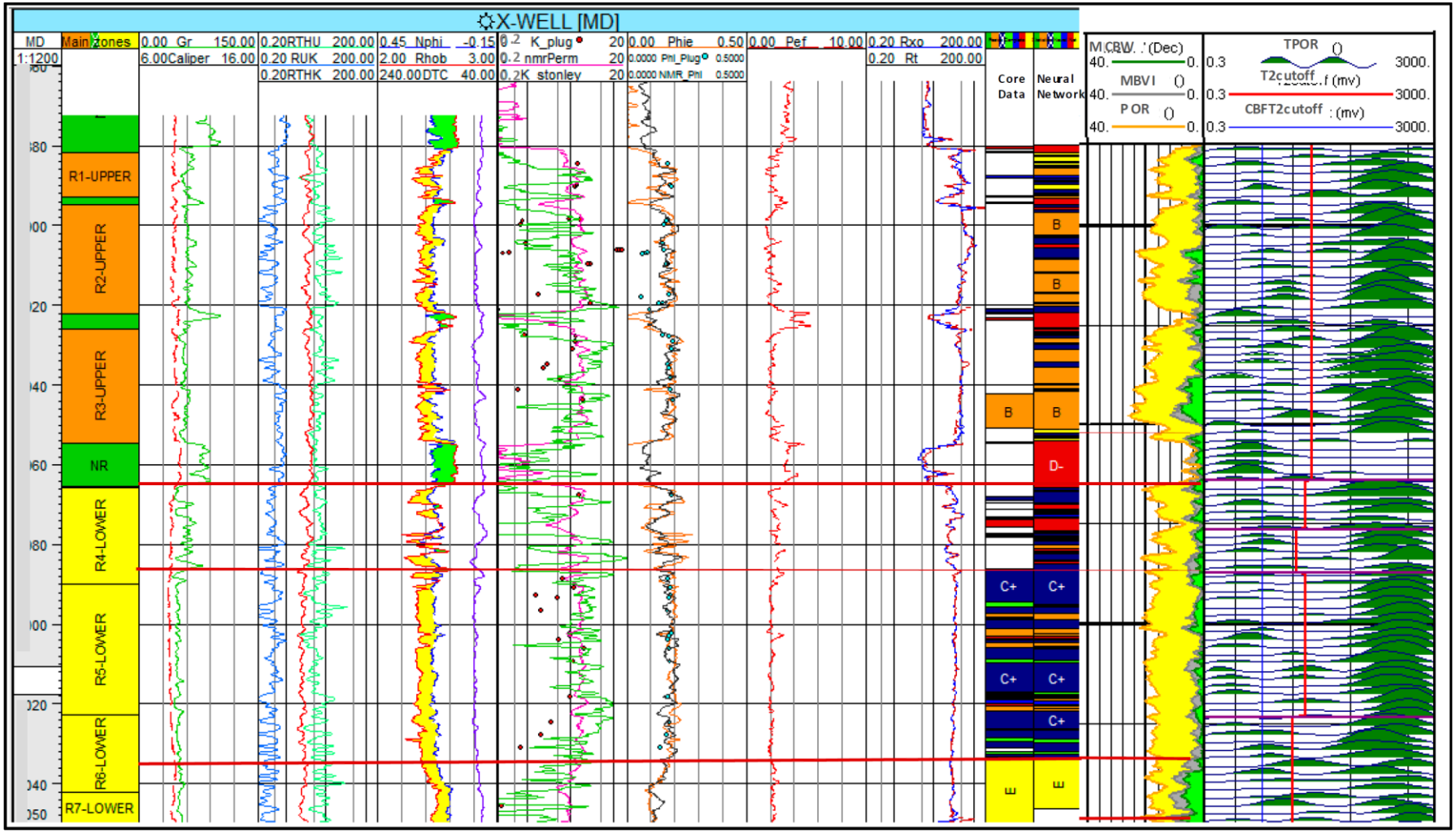

Figure 3. Well composite with main zones (track 2), sandstone shading (Nphi x RhoB track 5), permeability curves and core data (track 6), porosity (model curve in orange and NMR curve in black) and core data (track 7). The core facies are in track 10 and the neural network result in track 11. NMR T2cutoff adjusted in track 13.

Clay Type	CEC (meq/g)	ϕNphi (pu)	ρ avarage (g/cc)	Principal elements
Smectite	0.8-1.5	0.24	2.45	Na,Ca,Mg,Fe
Illite	0.1-0.4	0.24	2.65	K, Mg,Fe,Ti
Chlorite	0-0.1	0.51	2.8	Mg, Fe
Kaolinite	0.03-0.06	0.36	2.65	

Table 1. Clay CEC values, porosity, density and principal elements. (Source: Nascimento, 2007).

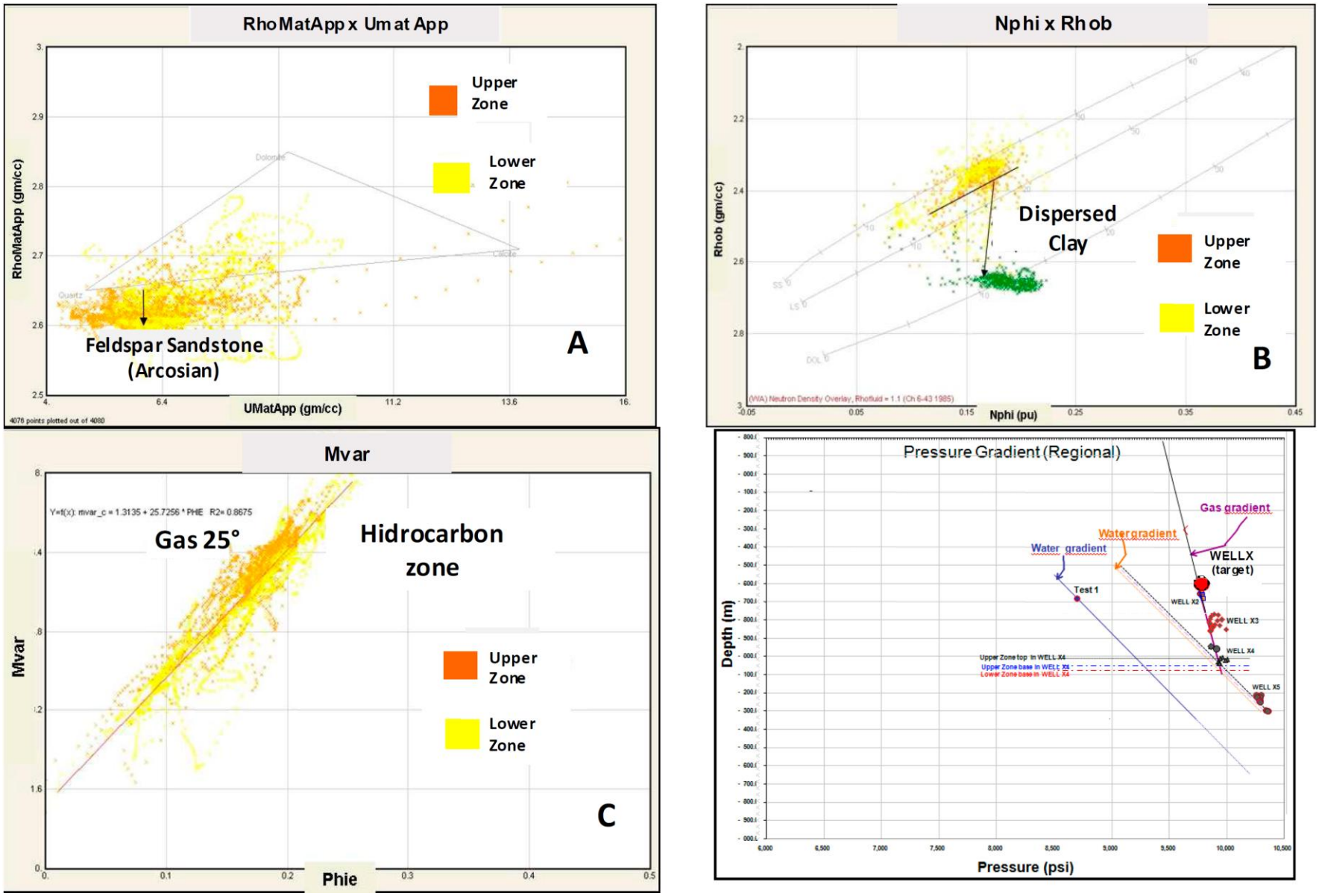

Figure 4. Crossplots analyzed. RhomatApp versus UmatApp (A), Nphi versus RhoB (B), Mvar versus Porosity (C) and Pressure data versus Depth (D). The crossplots A and B show that the reservoirs are composed by feldspar sandstones with dispersed clay essentially. The crossplots C and D show a gas saturated reservoir with no water contact.

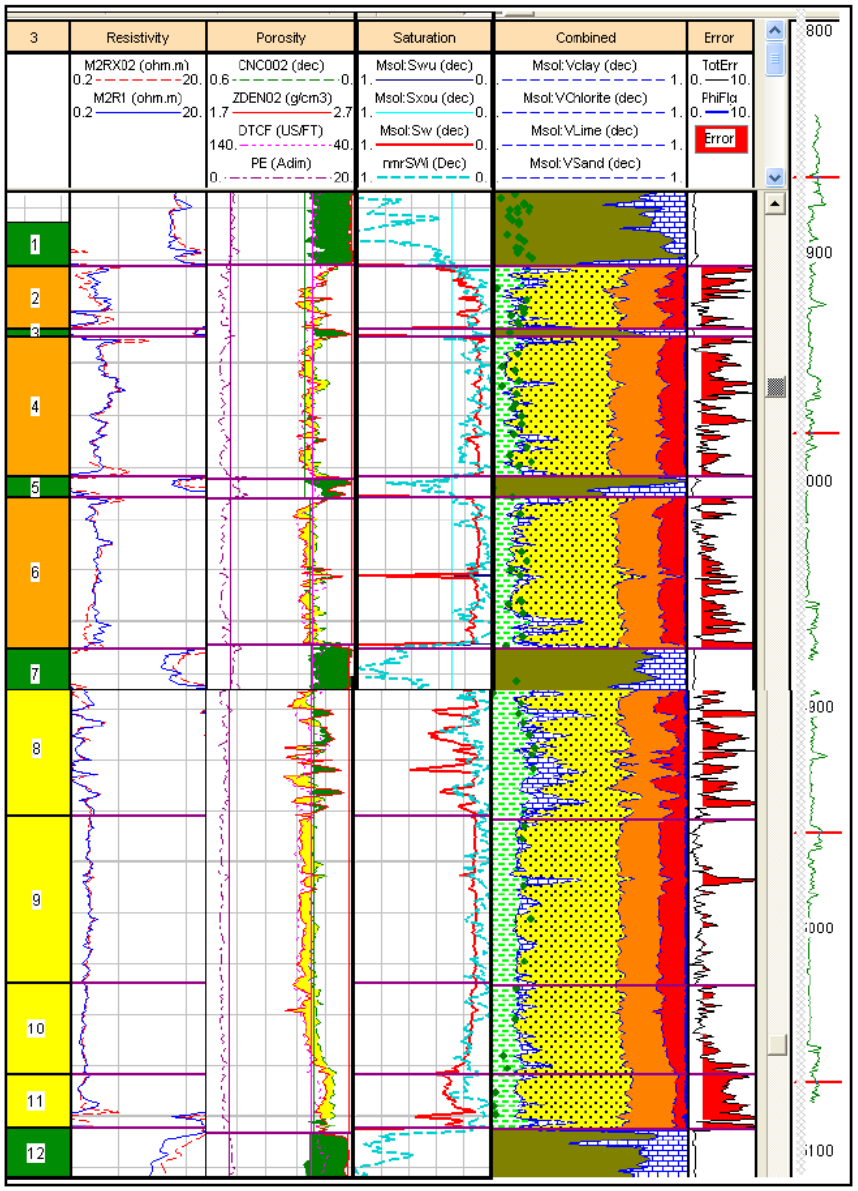

Figure 5. Probabilistic model composite. Track 4 (saturation track) shows the Sw from NMR (in cyan) and Sw from probabilistic model (in red) with good correlation. The track 5 (combined track) shows the mineralogical model, note that the chlorite plug data (green dots) fit perfectly with the chlorite curve modeled. The track 6 (error track) shows the error in the inversion model.

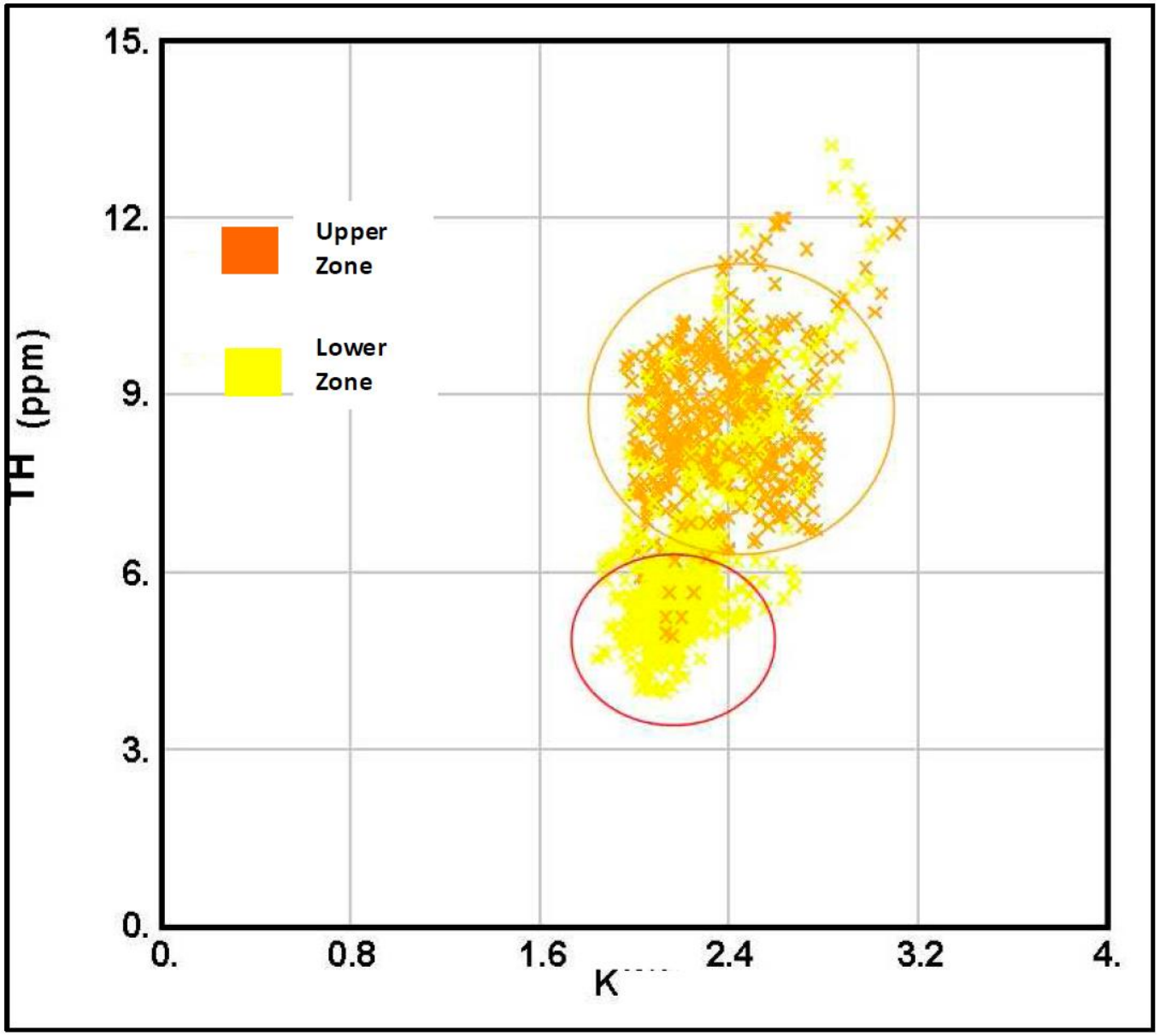

Figure 6. Th versus K crossplot. Note the separation between upper and lower zone.

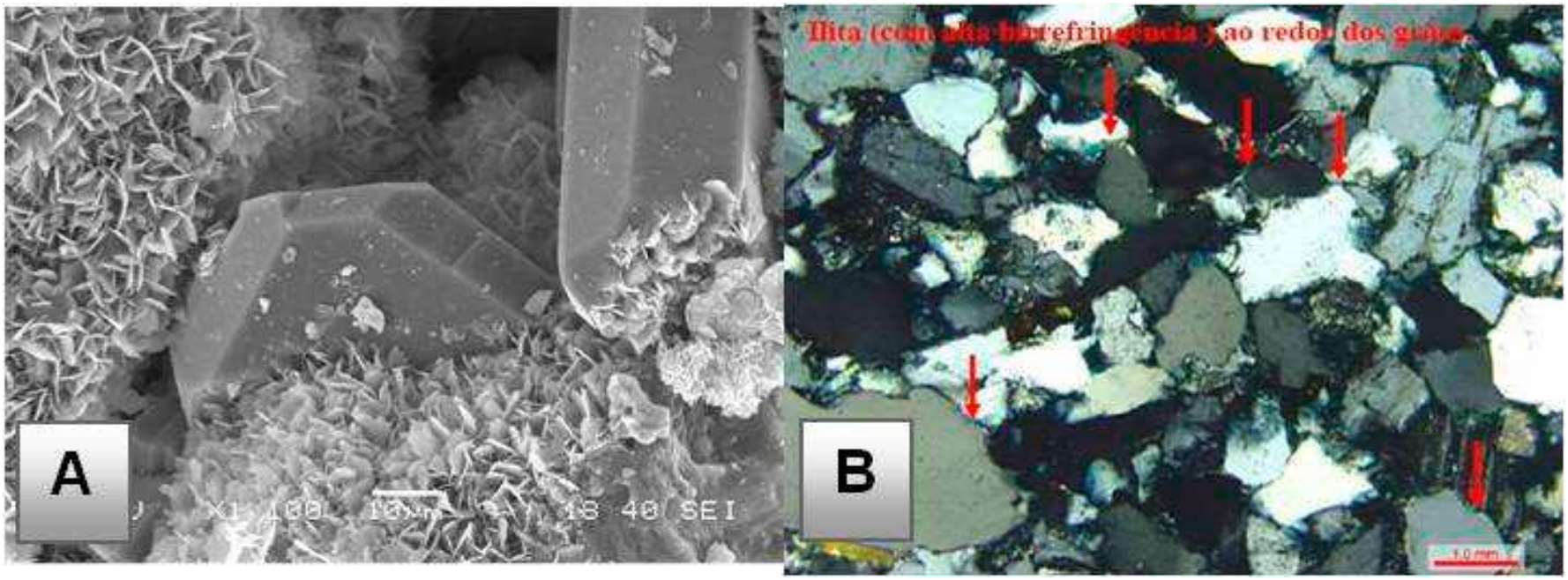

Figure 7. SEM image (Scanning Electron Microscopy) from Upper Zone showing chlorite (A). The second picture (B) shows microscopy image from Lower zone (Souza e Dias Filho, 2007).

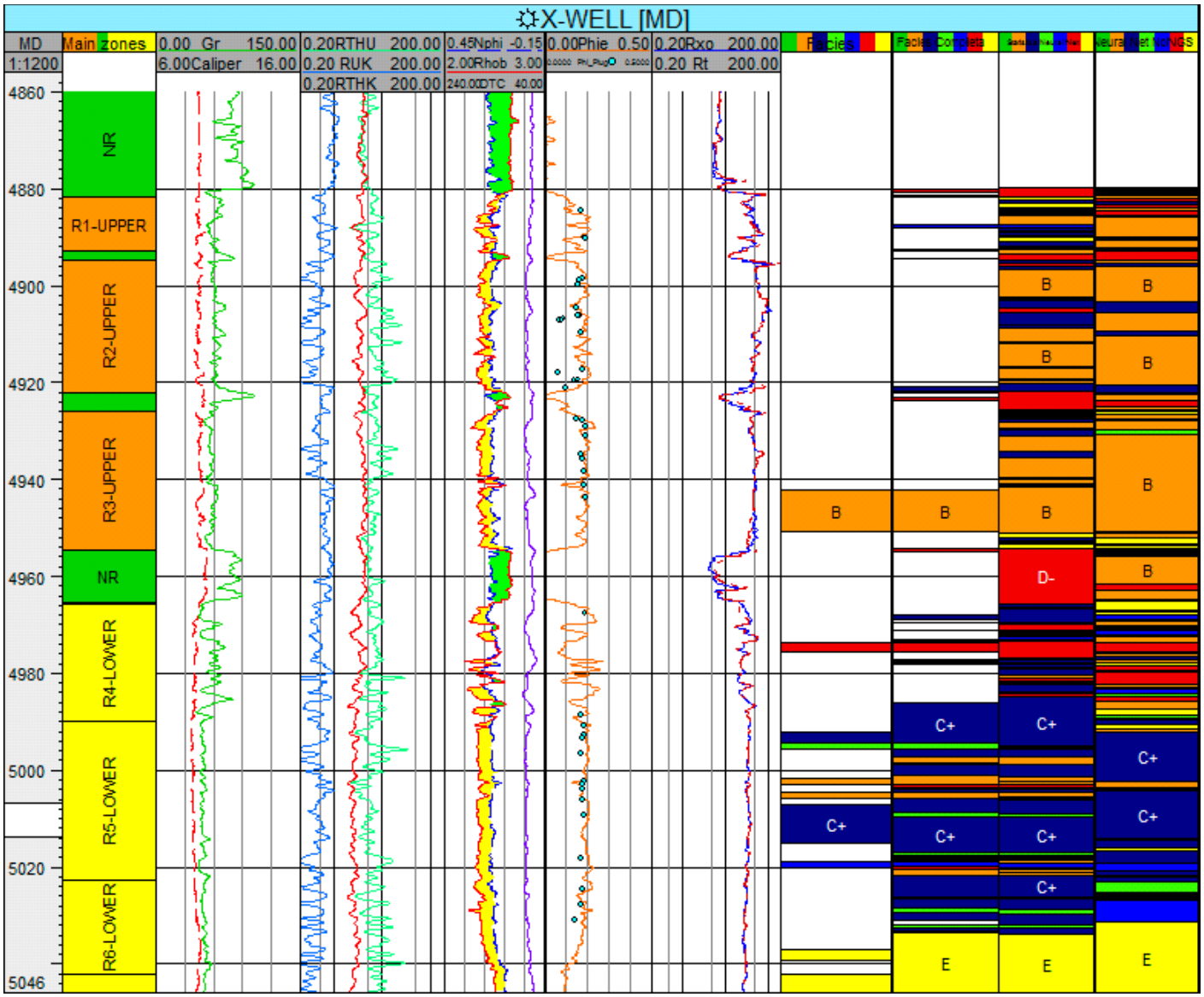

Figure 8. Well composite showing the neural networks. The track 8 shows the core data used to train the networks, the track 9 shows the complete core information and the last two tracks show different networks. The first one showed better result and took into account the NGS log curves while the last one was not so predictive and just had the conventional set of log curves as variable. Those networks used the same configuration and those are the best results for each input data.